MJSAT

Malaysian Journal of Science and Advanced Technology

journal homepage: https://mjsat.com.my/

Descriptive Design and Construction of a Hybrid Induction Cooker for Domestic Use in Sub-Saharan Africa

Rivaldo Poclaire Kengne Fotsing[1], and Narcisse Serge Nouadjep[1]*

[1]*Department of Electrical and Electronic Engineering, Faculty of Engineering and Technology, University of Buea. Buea, Cameroon.*

KEYWORDS

Induction cooking
Microcontroller
Solar powered
EMF
High Frequency

ARTICLE HISTORY

Received 24 May 2024
Received in revised form 23 June 2024
Accepted 27 July 2024
Available online 3 August 2024

ABSTRACT

This work details the design and implementation of a 24V, 0.48kW, 120kHz hybrid induction cooker that utilizes both solar and grid power sources, prioritizing solar energy. Relying on solar power is advantageous in regions of Cameroon with frequent power outages or no electricity, yet abundant solar irradiance, thereby addressing issues related to conventional cooking methods. The study involved designing various components and circuits necessary for building the system, such as the battery charger and automatic selection circuitry for switching between solar and grid power. Efficiency was evaluated by measuring power input and consumption. The output current and voltage waveforms were analysed to demonstrate the purity of the high-frequency alternating current. Comparative results indicated that using the induction cooker offers several benefits over traditional cooking methods, including faster cooking times, lower energy consumption, improved safety, and environmental friendliness.

1. INTRODUCTION

While culinary innovation progresses, a major challenge remains inefficient and unsustainable cooking methods. In developing countries like Cameroon, the reliance on wood, coal, and kerosene for cooking leads to significant problems. These traditional methods contribute to forest degradation, deforestation, and the emission of harmful pollutants, while also being inefficient [1,2]. Modern options such as gas and electric stoves have their drawbacks. Gas stoves release greenhouse gases, while electric stoves, although slightly more efficient and environmentally friendly, pose higher safety risks, including a greater incidence of fires [3]. For instance, the rate of reported fires per million households is 2.4 times higher with electric ranges, the civilian fire death rate per million households is 1.9 times higher, and the civilian fire injury rate per million households is 3.6 times higher compared to households using gas ranges [4].

Induction cookers present a potential solution by using electromagnetic fields to heat cookware directly, eliminating open flames and reducing energy consumption. This technology offers significant efficiency and safety advantages, transforming cooking practices and impressing both chefs and home cooks [5]. However, current research on induction cookers for developing regions reveals limitations. Most existing designs rely solely on grid electricity [6] or solar energy [7,8], and those that use both often lack integrated battery charging capabilities. Even "clean" gas fuels, despite some improvements, still produce pollutants and are finite resources [9], in addition to logistical issues in remote areas [10]. This poses a critical problem in regions with unreliable grid power and limited sunlight hours. Therefore, a cleaner and more sustainable cooking solution involves the use of both grid and solar energy, as exemplified in our approach.

This study endeavors to overcome these challenges by conceptualizing, simulating, and constructing an intelligent induction cooking setup tailored for use in Cameroon. Our inventive design integrates an automatic selection feature that effortlessly adjusts to the prevailing power supply, whether it be grid electricity or batteries charged via solar panels. This

*Corresponding author:
E-mail address: Narcisse Serge Nouadjep <nouadjep@gmail.com>.
https://doi.org/10.56532/mjsat.v4i3.328

compact device not only delivers enhanced efficiency and safety during cooking but also addresses the urgent issue of energy wastage in Cameroonian homes. By advocating for a clean and sustainable culinary approach, our objective is to foster a healthier environment and enhance the overall well-being of Cameroon's populace.

The configuration comprises a transformer for reducing mains voltage from 220V to 24V AC, a rectifier circuit for converting AC to DC, a tank circuit for transforming DC into high-frequency AC, a battery charger to replenish the battery using solar energy when accessible, a control circuit to regulate cooking timing, a fan for system cooling, and a pancake coil to generate the necessary electromagnetic fields.

2. METHODOLOGY

2.1 Design theories and working principle

The schematics for the different units, including the oscillatory, charge controller, and rectifier, were created and simulated using LTspice and Proteus. These designs consist of electronic components like MOSFET transistors, capacitors, inductors, resistors, diodes, LCDs, and keypads, all functioning together in harmony.

The analytical investigation of domestic induction heating systems is detailed in [6,11]. While gas and electric stoves remain prevalent in the Western market, induction heating for cooking applications is swiftly gaining ground across Europe, especially for smaller cooking vessels [12]. Induction cooking technology not only outperforms traditional solutions like gas and electric stoves in terms of efficiency conversion but also offers advantages such as rapid heating, localized spot heating, direct heating, high power density, reliability, low operational costs, and minimal noise [13]. According to the U.S. Department of Energy, these systems boast an energy transfer efficiency of approximately 59.46-81.78%, compared to 63.86 -74% for non-induction electric units with smooth tops, resulting in approximately 10 to 15% energy savings for the same heat transfer [14]. Electromagnetic induction refers to the phenomenon wherein a changing magnetic field induces an electric current or electromotive force (EMF) in a conductor. This fundamental principle, initially observed by Michael Faraday in the early 19th century, serves as the foundation for the operation of numerous electrical devices and technologies, including transformers, electric motors, and generators [15,16].

An induction heater comprises an induction coil, typically crafted from copper or another conductive material, supplied with high-frequency alternating current (AC). As this AC flows through the coil, it generates a fluctuating magnetic field around it. This varying magnetic field induces eddy currents within a nearby conductive ferromagnetic material, commonly a metal object. These eddy currents, in turn, lead to resistive heating within the material due to its electrical resistance. This heating process ensues because the eddy currents encounter resistance as they circulate within the conductive material, resulting in rapid and uniform heating [4]. The heat generated is directly proportional to the square of the current multiplied by the resistance of the metal. Given that the load metal is typically composed of iron, the resistance for iron is considered in the analysis as shown in Figure 1.

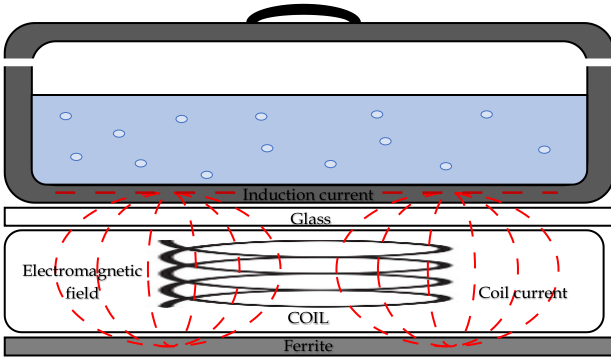

Fig. 1. Illustration of induction heating process

2.2 Inverters Specifications

Electronic switches such as diodes, SCR (thyristors), IGBTs, MOSFETs, and BJTs are integral components in various power conversion circuits, tailored to meet the specific demands of the load [17]. In the design of inverters, these switches serve the purpose of converting DC power into AC power. While DC represents a relatively stable and positive voltage source, AC fluctuates around a reference base level, typically in a square or sinusoidal waveform [18]. The conversion of DC input to AC output is achieved by controlling the switching of these switches at different intervals, resulting in a pulsating output that may contain harmonic components. However, proper control schemes can mitigate these harmonics. In our scenario, the inverter may adopt either a half-bridge or full-bridge configuration, contingent upon the arrangement of switches employed as in Figure 2.

The half-bridge series-resonant topology presents several advantages over the full-bridge resonant topology. In our case, it offers simplicity by requiring fewer components and being easier to control. This simplicity not only streamlines the design process but also contributes to enhanced reliability by reducing stress on components, all while maintaining high efficiency suitable for cooking applications. Moreover, its straightforward design facilitates easier control and tuning for optimized induction heating. Additionally, its cost-effectiveness is attributed to its reduced component count and uncomplicated design.

2.3 LC Tank Circuit (Oscillator)

An oscillator refers to an electronic circuit or apparatus responsible for producing an electrical waveform or signal characterized by a defined frequency and shape [17]. It finds widespread application across diverse electronic systems and devices demanding stable and repetitive waveforms. For instance, oscillators are integral components in computers, clocks, watches, radios, and metal detectors, among various other devices. Numerous designs of oscillator circuitries exist, including the Harley, Colpitts, LC tank, and others. Additionally, integrated circuits (ICs) can be tailored to generate stable or oscillating outputs. Figure 3, illustrates an LC tank circuit, for visual reference.

When the switch transitions from point A to B, an energy exchange occurs between the inductor (L) and the capacitor (C). Initially, the voltage across the capacitor begins to decrease as the current flowing through the coil starts to increase. This increasing current generates an electromagnetic field surrounding the coil, which opposes the flow of current. As the capacitor discharges completely, the energy initially stored in

the capacitor as an electrostatic field is transferred to the inductive coil (*L*) in the form of an electromagnetic field around the coil's windings.

With no external voltage present in the circuit to sustain the current within the coil, the current begins to decline as the electromagnetic field collapses. A back electromotive force (emf) is induced in the coil (e = -Ldi/dt), maintaining the current flow in the original direction [19]. These current charges the capacitor with the opposite polarity to its initial charge. The capacitor continues to charge until the current diminishes to zero, and the electromagnetic field of the coil completely collapses. Consequently, the energy initially introduced into the circuit via the switch is returned to the capacitor, which once again holds an electrostatic voltage potential across it, albeit of the opposite polarity. Subsequently, the capacitor begins to discharge again through the coil, restarting the entire process [19]. This cycle repeats itself. The resonant frequency (*F*) is determined using the formula expressed in (1).

$$F = \frac{1}{2\pi\sqrt{LC}} \tag{1}$$

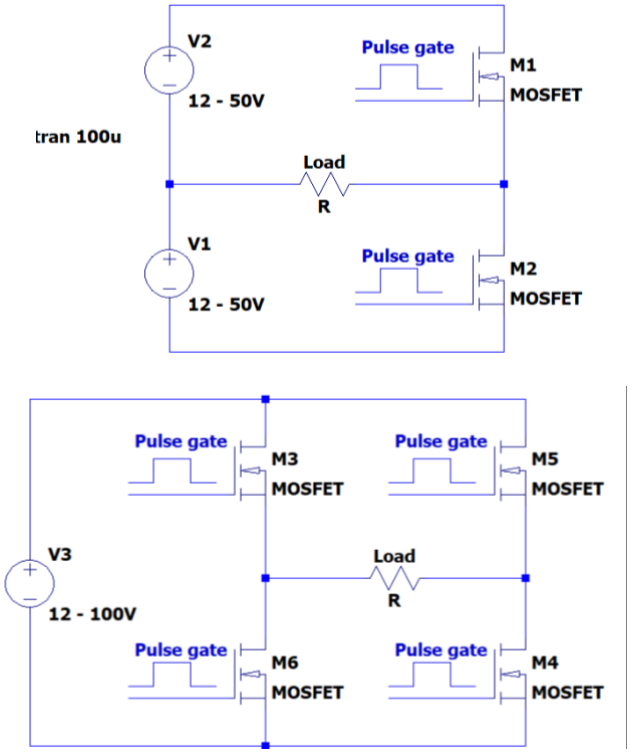

Fig. 2. Half-bridge series-resonant topology and full-bridge hybrid resonant inverter

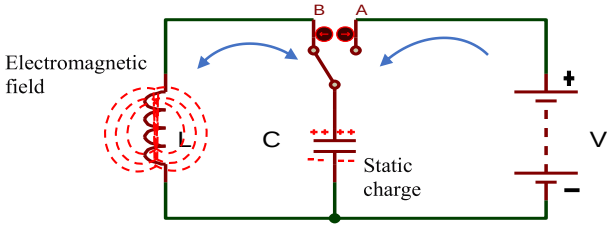

Fig. 3. LC Tank Circuit

2.4 *Battery Charger*

The 24V 10A battery charger is tasked with replenishing the battery, drawing power from either the solar panels or the mains electricity. Its components comprise distinct sections, including the Input Power Source, Switching and Control Sections, Current-Limiting Circuit, and Soft-Start Circuit. Figure 4 shows the battery charger circuitry.

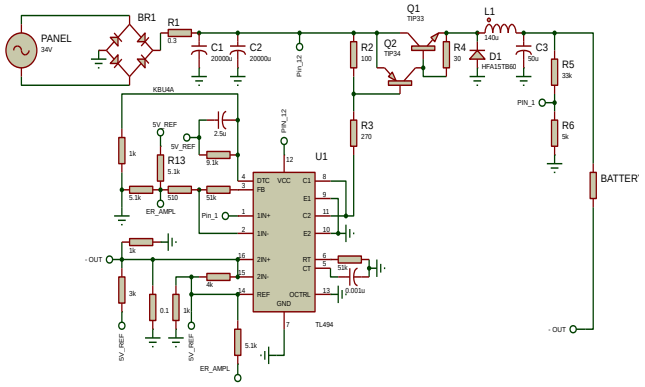

Fig. 4. Battery charger circuit

2.5 *Design Parameters and Criteria*

The concept behind designing a half-bridge resonant induction cooker focuses on achieving efficient and precise control of the induction heating process, while also prioritizing reliability and cost-effectiveness. This design encompasses several crucial factors, including the optimization of the resonant tank circuit—comprising the inductor and capacitor—to effectively generate high-frequency AC power for induction heating. Careful consideration is given to the configuration of the half-bridge, which includes switches and resonant components, to minimize losses, improve power transfer efficiency, and enable precise control over the heating process. Control strategies, such as employing hard switching techniques, are integrated to regulate the delivery of power to the cooking vessel, ensuring consistent and uniform heating. In summary, the design approach for a half-bridge resonant induction cooker emphasizes achieving peak efficiency, precise control, reliability, and adherence to cost-effective principles. The induction coil is used in parallel with the capacitor to generate the electromagnetic field.

a) *Sizing the pancake coil (induction coil)*:

The determination of the coil's number of turns primarily relies on the diameter of the conductor piece and the spacing between the coil windings as in (2). Considering the coil's application for a limited area, a decision was made to utilize 8 turns.

$$N = \frac{R_{out} - R_{in}}{D_{con} + S} \tag{2}$$

Where,

N = number of turns of the coil

R_{out} = outer radius of work coil (m)

R_{in} = inner radius of work coil (m)

D_{con} = coil diameter

S = spacing

Overall coil length is calculated as in (3)

$$l_{coil} = \pi N (R_{out} - R_{in}) \quad (3)$$

Table 1 highlights the conductor characteristics.

Table 1: Characteristics of the conductor used

Specification	Value	
Material	Copper	Aluminium
Resistivity (Ωm)	$1 \cdot 7 \times 10^{-8}$	$2 \cdot 82 \times 10^{-8}$
Relative permeability	1	1
Number of strands	28	3

b) *Calculation of Operating Frequency)*:

The maximum frequency can be approximately estimated at the characteristic point of individual strands as in (4), where the skin depth is equal to the radius of strand *Rs*.

At $f = f_{max}$, $R_s = \delta$

$$f_{max} = \frac{\rho}{\pi \mu_0 R_s^2} \quad (4)$$

When the radius of the solid wire or the equivalent bundle wire (r_b) is equal to the skin depth, the frequency is very low. At $f = f_{max}$, $r_b = \delta$

$$f_{min} = \frac{\rho}{\pi \mu_0 R_s^2} \quad (5)$$

Where ρ = electrical resistivity of the cookware,

μ_0 = permeability of air

c) *Calculating the Inductance*:

Inductance is obtained as per (6) and (7).

$$L = \frac{N^2 \times A^2}{30A - 11D_i} \quad (6)$$

$$A = \frac{D_i + N(D_w + S)}{2} \quad (7)$$

Where: D_i = inner diameter, D_w = wire diameter, and A = average diameter of the coil in mm,

With all considerations and calculations, plugging the values in the inductance formula in equation (6), (based on the Harold A. Wheeler approximation), an inductance of 6uH is obtained.

d) *Calculation of the resonant frequency*:

The resonant frequency of the oscillating circuit is determined by the resonant capacitor and the work inductor coil. The inductance has been measured at 6uH, and resonance happens when the reactances of these two components are equal. That is,

$$XL = XC \quad (8)$$

This will imply that

$$L\omega = \frac{1}{C\omega}, \Rightarrow \omega^2 = \frac{1}{LC}, \Rightarrow f = \frac{1}{2\pi\sqrt{LC}} \quad (9)$$

For the inductance, we computed the maximum and minimum frequencies (using equations (3) and (4)) that are suitable for our system. We cannot select a resonant frequency below 20kHz because such low-frequency oscillations would be audible and unpleasant to the human ear. Therefore;

$$C = \frac{1}{L\omega^2} = \frac{1}{L(2\pi f)^2} \quad (10)$$

2.6 Design Analysis

The block diagram in Figure 5 illustrates all the different components of the system. The induction cooker system comprises several key components: an AC-DC converter, a driver and LC Tank circuit, a control circuit, a battery charger, and the load. The AC-DC converter features a 220-24V AC, 15A transformer, along with rectifying diodes and filtering capacitors, to adjust the voltage for the system. The driver and LC Tank circuit use MOSFET semiconductor switches to generate oscillations within the LC Tank circuit, facilitating energy transfer to the load. This oscillation is maintained by a feedback loop. The control circuit includes relays for automatic switching and a microcontroller to regulate cooking times. Additionally, a dedicated battery charger supports battery charging via solar panels. Finally, the load, represented by the cookware, is placed on an induction coil (pancake coil), which receives the transferred energy within the system.

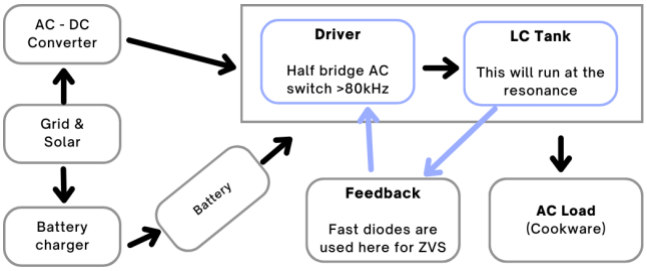

Fig. 5. Overall System block diagram

Figure 6 illustrates the operational sequence flow chart, detailing the steps involved in the cooking process. It begins with user input, followed by cooking time control and monitoring, and includes safety mechanisms.

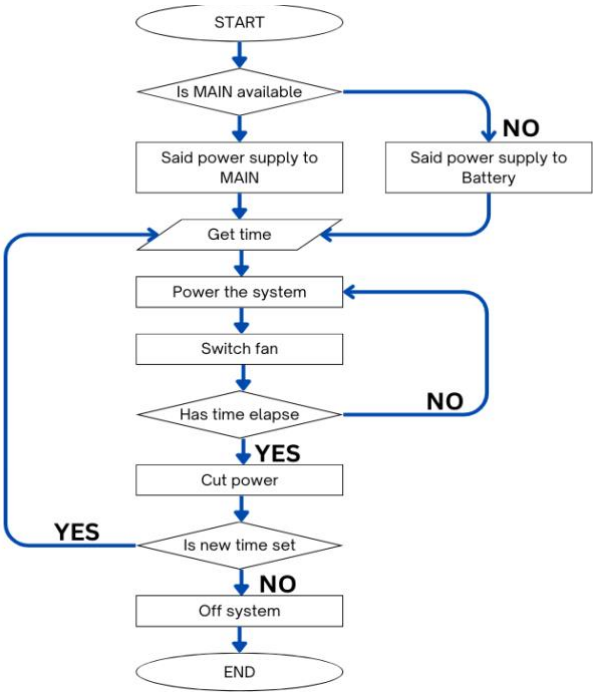

Fig. 6. System flow chart

The oscillatory circuit (Figure 7) and the control circuit (Figure 8) were designed using Proteus software version 8.16.

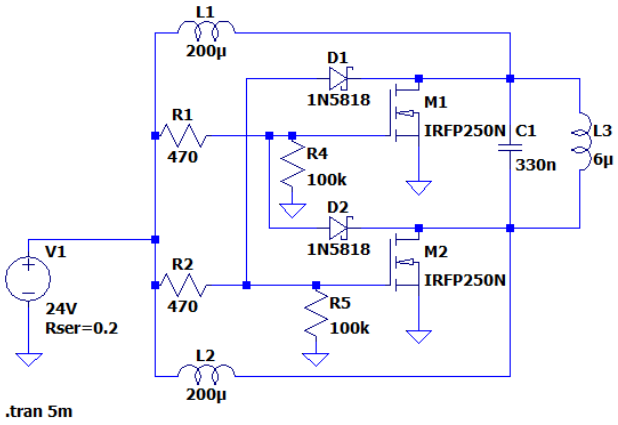

Fig. 7. Oscillatory circuit diagram

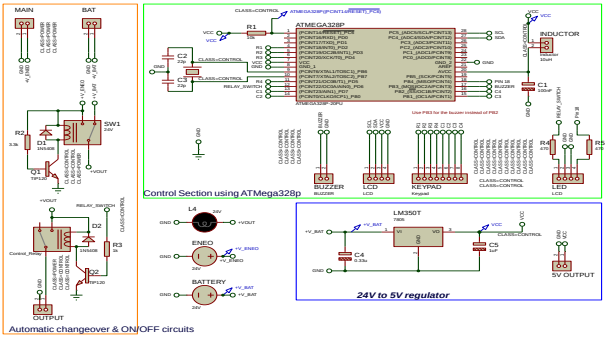

Fig. 8. Complete control circuit

The automatic changeover segment handles the transition between battery power and the main electrical supply. When solar irradiance is insufficient, the "Automatic Change Over ON/OFF" feature will switch to grid power to ensure a continuous supply for the device and to charge the batteries. This process occurs automatically, with a priority set on solar power to reduce dependency on the grid. The control segment utilizes an ATMEGA microcontroller to manage timing and oscillator switching, while a regulator section steps down the voltage from 24V to 5V to power the controller. The user interface encompasses both the output (display) and input (keypad). Figure 9 illustrates the simulation of how the circuit operates.

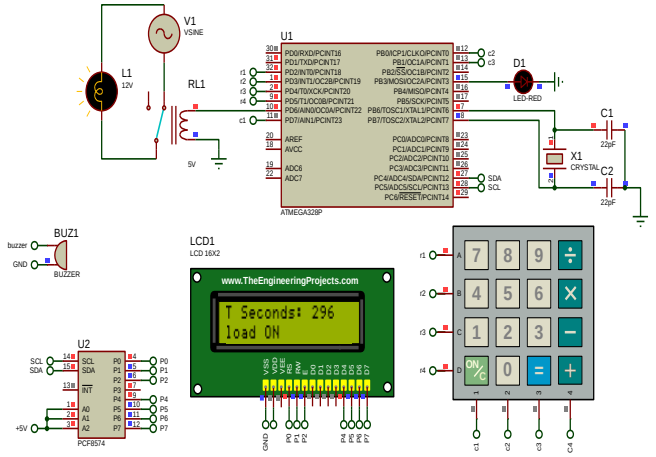

Fig. 9. User interface

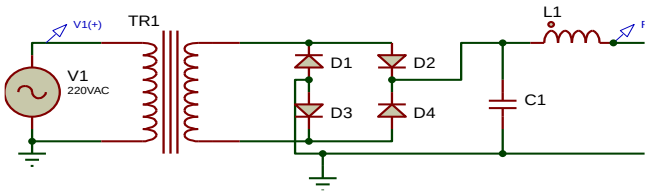

Fig. 10. Rectifier circuit

3. RESULTS AND DISCUSSIONS

3.1 Voltage profile for the LC tank circuit and the gate

The voltage profiles illustrated by Figure 11 and Figure 12 respectively are for the LC tank circuit and at the gate of both MOSFET. Figure 11a illustrates the voltage profile of the tank circuit, which displays a transient voltage (spike) right after the system is powered. This spike is caused by the initial mismatch between the applied voltage and the reactive response of the inductor and capacitor. It represents the circuit's dynamic adjustment towards reaching a stable operating point. Figure 11b shows a zoomed portion of the voltage profile with the voltage amplitude after the surge has stabilized. Leveraging the principle of resonance, a high-frequency oscillation is used to create the magnetic field, ensuring efficient energy transfer, stable operation, and overall effectiveness of the induction cooking process.

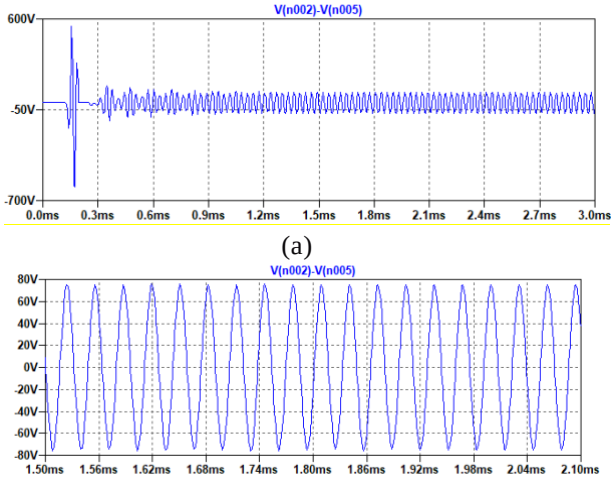

Fig. 11. Voltage waveform of the oscillatory circuit

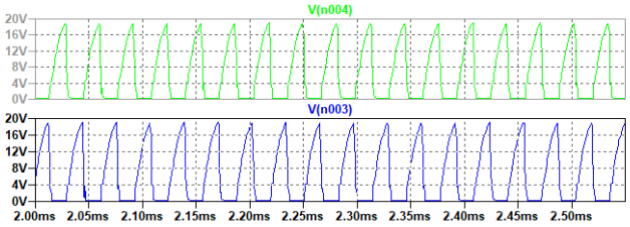

Fig. 12. Signal at the gate of both MOSFET

The gate voltage shifts sequentially, one following the other, during the switching process. Complementary signals control the two MOSFETs, so when one MOSFET is turned ON (with a gate voltage of 18V), the other is turned OFF (with a gate voltage of 0V), and vice versa. This setup ensures a continuous path for current to flow through the inductor, maintaining uninterrupted oscillation.

3.2 Voltage profile and output waveform of the rectifier circuit

In the setup, direct power from the grid was utilized as a secondary source, providing 220V AC, which is then stepped down and rectified to app`roximately 24V DC before passing through the tank circuit as shown in Figure 13.

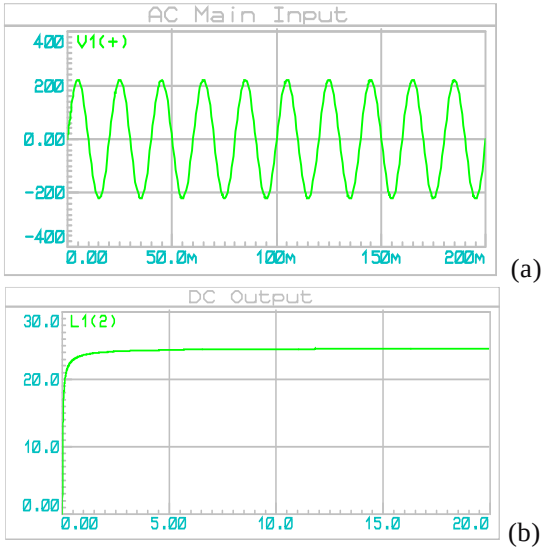

Fig. 13. (a) Input voltage from the grid, (b) Output DC waveform after rectification

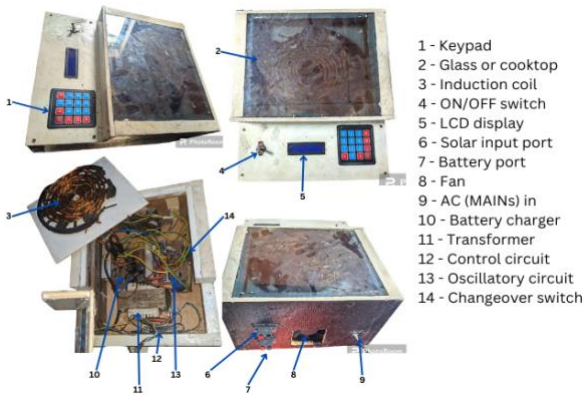

Fig. 14. External and internal view of the system

3.4 Load test for input and output power (grid) using water as a sample

The load tests are expressed in Table 2 and Table 3 respectively for the input power and the output power. The values presented in Table 2 were derived from measuring voltage and current for varying amounts of water and heating durations. The results demonstrate a low power output, attributed to the input voltage (Vin) being only 147-155VAC rather than the expected 220-230VAC from the grid at the time of testing. Consequently, this caused the system to require more time to heat the cookware. The value 7.85W obtained at no load (cookware absent) is the power loss in the system due to internal resistances and switching losses, transformer losses and AC-DC converter.

Similarly, values presented in Table 3 were derived from measuring voltage and current at the coil level (output). A power loss of 20.16W is observed which is due to the internal resistances, inverting losses, and coil level losses in addition to the losses mentioned above.

3.5 System efficiency

The output power is utilized to calculate the system's efficiency. The efficiencies for 3, 6, and 10 minutes are calculated below using (11).

$$\eta = \left(\frac{Pout}{Pin}\right) * 100\% \tag{11}$$

η_{3min} = 79.98% η_{6min} = 80.27% η_{10min} = 82.95%

Therefore, overall efficiency is η = 81.07%

The oscillatory circuit oscillates at a frequency of 100kHz to 120kHz.

3.6 Discussion

The developed prototype achieved an efficiency of 81.07%. Although this is slightly higher than that of some traditional cookers (72.2 – 77.6% for small and large vessel mentioned by Micah et al.,[12]) such as gas, it falls short of the peak efficiency (ranging from 69% to 95%) reported in some traditional and commercial induction cookers according to other research articles [6,8,9]. This efficiency is also slightly inferior compared to 81.78% for a 1800W mentioned by Aisyah et al., [14]. This discrepancy can be attributed to differences in components, design, and technology. The use of a 24V DC

input limited the cooking speed compared to commercial models that utilize higher power inputs for faster heating. However, the prototype offers a unique advantage by integrating solar power as the primary energy source when sufficient battery power is available, with the grid serving as a backup. This feature distinguishes it from most commercially available induction cookers (as highlighted in Table 4), which rely solely on grid electricity [20,21]. The complexity introduced by solar integration resulted in higher costs compared to both commercial induction cookers and traditional methods. Furthermore, the use of locally sourced materials in the prototype led to a larger size compared to the more compact designs achieved with highly integrated materials in commercial models. Additionally, the prototype featured only a single power level, whereas commercial options often offer multiple power settings.

4. CONCLUSION

This study successfully designed and implemented a 24V, 0.48kW, 120kHz hybrid induction cooker that prioritizes solar energy while also integrating grid power as a secondary source. The system is particularly beneficial for regions in Cameroon Sub-Saharan Africa) where power outages are common, or electricity access is limited, but solar irradiance is plentiful. The research involved the development of essential components (such as the battery charger and an automatic switching circuit between solar and grid power, ensuring reliable operation under varying conditions.

Efficiency assessments demonstrated the hybrid induction cooker's effective utilization of solar power, optimizing energy use by seamlessly switching to grid power when solar energy is insufficient. Analysis of output current and voltage waveforms confirmed the purity of the high-frequency alternating current produced, essential for efficient induction cooking.

Key innovation was the integration of an auto-selection mechanism and a battery charger, enabling seamless switching between grid electricity and solar-charged batteries. This feature addresses a critical gap in many existing solar-powered induction cookers, which lack battery charging capabilities.

Table 2. Load test for the input power from the grid

With no load						
V_{in} (V)			**I_{in} (A)**		**Power (W)**	
157			0.05		7.85	
With load						
Time (min)	**V_{in} (V)**	**I_{in} (A)**	**AC Power P_{in} (W)**	**Initial Temp (°C)**	**Final Temp (°C)**	**Qty of H_2O (ml)**
3	155	1.31	203.05	28	62	125
6	155	1.25	193.75	29	62	250
10	147	1.23	180.81	29	80	125

Table 3. Load test for the output power in the coil

With no load						
V_{in} (V)			**I_{in} (A)**		**Power (W)**	
32			0.63		20.16	
With load						
Time (min)	**V_{in} (V)**	**I_{in} (A)**	**DC Power P_{out} (W)**	**Initial Temp (°C)**	**Final Temp (°C)**	**Qty of H_2O (ml)**
3	29.0	5.6	162.4	28	62	125
6	28.8	5.4	155.52	29	62	250
10	28.3	5.3	149.99	29	80	125

Table 4. Comparison of the design cooker with the commercialized one

	This System	**Others (Commercial and traditional)**
Efficiency	81.07%	70 – 90%
Cooking speed	A 24V DC input voltage (0.48kW max output) limits the heating speed.	The input voltage is 310V DC after rectification giving it higher power and faster heating speed [20,21].
Solar power integration	Its main source is solar when there is enough power in the battery with the grid as a backup making the system unique among many.	Most commercial induction cooker uses direct grids only and other prototypes use solar only [22].
Cost and system complexity	Due to solar integration, the system turns out to be more complex and expensive.	More affordable due to their simplicity
Power Levels	Single power level	Multiple power levels
Size	Bigger in size due to the use of locally sourced material and its complexity.	Smaller due to the highly integrated material used.
Battery charger	Has in integrated battery charger.	Do not have.

Consequently, this innovative approach addresses the immediate challenges of conventional cooking methods and promotes sustainable and reliable cooking solutions in areas with inconsistent electricity supply. This study highlights the

potential of hybrid induction cookers to enhance quality of life while supporting environmental sustainability.

REFERENCES

[1] Wright, Caleb, Sathre, Roger; et al.: "The global challenge of clean cooking systems," Food Security, 2020. International Society for Plant Pathology and Springer Nature B.V. doi:10.1007/s12571-020-01061-8.

[2] Moresi, Alessio C. and Mauro: "Environmental impact of the main household cooking systems—A survey," Italian Journal of Food Science 34 (1), p. 86 –113, 23 February 2022. doi:10.15586/ijfs.v34i1.2170.

[3] Ashlinn K., Nigel B., Elisa P. et al.: "An analysis of efforts to scale up clean household energy for cooking around the world," Energy for Sustainable Development 46, July 2018. DOI:10.1016/j.esd.2018.06.011.

[4] McGree, Shelby H., Tucker: "Home Cooking Fires," National Fire Protection Association (NFPA), Research, 01 September 2023.

[5] Hope, Mary H.J. Farrell and Paul: "CR's Complete Guide to Induction Cooking," October 6, 2022, Updated October 11, 2022.

[6] Emilio P., Jesús A., Ignacio L., et al.: "Design methodology of high performance domestic induction heating systems under worktop," IET The Institution of Engineering and Technology 2019, no. 13 Iss. 2, pp. 300-306, 01 February 2020. doi: 10.1049/iet-pel.2019.0693.

[7] Juan P., Valceres V., Fernando L.: "Household induction cooking system based on a grid-connected photovoltaic system," IET © The Institute of Engineering and Technology, no. 14 Iss. 8, pp. 1117-1128, 2020. doi: 10.1049/iet-cds.2019.0305.

[8] Egwaile J., M.O., and Oyedoh: "Design and Construction of A Solar Based Induction Cooker," Trans. of NAMP, Transactions of the Nigerian Association of Mathematical Physics, vol. 9, pp. 153-162, 2019.

[9] Wenxue G., Yingjie H., Rongsong Y., et al.: "Comprehensive Review on Thermal Performance Enhancement of Domestic Gas Stoves," ACS Omega, pp. 26663-26684, July 20, 2023.

[10] Lombardi F., Riva F., Sacchi M., et al.: "Enabling combined access to electricity and clean cooking with PV-microgrids: new evidences from a high-resolution model of cooking loads," Energy. Sustain. Dev, pp. 78-88, 2018, 49.

[11] Sergey A., Primiani, Graziano C. et al.: "Rigorous Electromagnetic Modelling Of Domestic Induction Heating Systems," UNIVPM, 2011.

[12] Micah S., Jeff D., Brian F., Frank S., "Induction Cooking Technology Design and Assessment Electric Power Research Institute (EPRI)," 2014 ACEEE Summer Study on Energy Efficiency in Buildings.

[13] ÓSCAR L., JESÚS A., CLAUDIO C., et al.: "Induction Heating Appliances: Toward More Flexible Cooking Surfaces," IEEE Industrial Electronics Magazine, 7(3), pp. 35 - 47, September 2013. doi:10.1109/mie.2013.2247795.

[14] S Aisyah, M Triani and R Rasgianti: "Energy efficency analysis for various type of electric cooker," in Annual Conference on Science and Technology, April 2021. doi:10.1088/1742-6596/1869/1/012175.

[15] Henry Semat and Robert Katz, "Chapter 32: Electromagnetic Induction," Physics, Research Papers in Physics and Astronomy.

[16] David H., Robert R., Jearl W.: “Fundamentals of Physics, Volume 1,” 10th edition.

[17] Ned M., Tore M., William P.: “Power Electronic Converters Applications, and Design,” 3rd edition, 2002.

[18] Rashid, Muhammad H.: “Power Electronics Handbook.”, 2011

[19] Hesborn A., Willis J., Franklin M. et al.: "A Review of Cooking Systems and Energy Efficiencies," American Journal of Energy Engineering, Mar. 22, 2021. doi:10.11648/j.ajee. 20210901.11

[20] Arthur K. K. Wong, N. K. Fong: "Experimental study of induction cooker fire hazard," school of engineering of Sun Yat-sen University, 2013. doi:10.1016/j.proeng.2013.02.098.

[21] Meenakshi S., Lokesh S., Sundaramahalingam S.: "Solar Powered Induction Cooking System," in 2nd International Conference on Power and Embedded Drive Control (ICPEDC), 2019. doi: 10.1109/icpedc447771.2019.9036681.

[22] Hesborn R., Willis J., Franklin M., et al.: "A Review of Cooking Systems and Energy Efficiencies," American Journal of Energy Engineering, Mar. 22, 2021.